The Importance of Dihydrogen Complexes $H_nGe(H_2)^+$ ($n = 0,1$) to the Chemistry of Cationic Germanium Hydrides: Advanced Theoretical and Mass Spectrometric Analysis

Phillip Jackson,[b] Nadja Sändig,[a] Martin Diefenbach,[a] Detlef Schröder,[a] Helmut Schwarz,*[a] and Ragampeta Srinivas[c]

Abstract: Investigations of $[Ge,H_n]^{-/0/+}$ ($n = 2,3$) have been performed using a four-sector mass spectrometer. The results reveal that the complexes $H_nGe(H_2)^+$ ($n = 0,1$) play an important role in the unimolecular dissociation of the metastable cations. Theoretical calculations support the experimental observations in most instances, and the established view that the global minimum of $[Ge,H_2]^+$ is an inserted structure may need reexamination; CCSD(T,full)/cc-pVTZ//CCSD(T)/6-311++G(d,p) and B3LYP/cc-pVTZ studies of three low-lying cation states ($^2A_1$ $HGeH^+$, $^2B_2$ $Ge(H_2)^+$ and $^2B_1$ $Ge(H_2)^+$) indicate a very small energy difference (ca. 4 kcal mol^{-1}) between $^2A_1$ $HGeH^+$ and $^2B_2$ $Ge(H_2)^+$; B3LYP favours the ion–molecule complex, whereas coupled-cluster calculations favour the inserted structure for the global minimum. Single-point multireference (MR) averaged coupled-pair functional and MR-configuration interaction calculations give conflicting results regarding the global minimum. We also present theoretical evidence indicating that the orbital-crossing point implicated in the spin-allowed metastable dissociation $HGeH^{+*} \rightarrow Ge(H_2)^{+*} \rightarrow Ge^+ + H_2$ lies above the H-loss asymptote. Thus, a quantum-mechanical tunneling mechanism is invoked to explain the preponderance of the H_2-loss signal for the metastable ion.

Keywords: ab initio calculations · dihydrogen complexes · germanium · hydrides · ion–molecule reactions · mass spectrometry

Introduction

Element hydrides are amongst the simplest chemical entities to examine theoretically and spectroscopically. Due to the uncomplicated nature of the sigma-bonding interaction hydrogen shares with heavier elements and coordination centres, hydride studies have often been used to elicit periodic and/or group trends. According to Squires, M–H bond strengths (M = transition metal) can be derived from an appreciation of the metal's electron affinity alone.[1] Investigations on metal hydrides have also contributed significantly to the understanding of the effects of heavy nuclei on molecular electronic structure.[2–6]

Pertaining to relativistic effects and group trends, hydrides of the heavy Group IV A elements have been the subject of a number of theoretical investigations;[6–10] however, there is still limited experimental information available for the heavy-atom substituted MH_n, $n = 1-3$. This can probably be attributed to the difficulty of preparation and handling of the heavier tetrahydrides (both SiH_4 and SnH_4 spontaneously ignite in air [11]) from which it is relatively simple to derive the lower hydrides. In spite of their significance to the chemistry of semiconducting film preparation, GeH_2 and GeH_3 as well as their ions have only recently attracted the attention of experimentalists.[12–16] Of paramount importance is the unimolecular dissociation of XH_4, X = Si, Ge [Eq. (1)], which has

$$XH_4 \longrightarrow XH_2 + H_2 \qquad (1)$$

been studied at very high levels of theory.[7] The reactions of neutral GeH_2 with a number of simple molecules have also been monitored,[14, 16] while selected charge-induced condensation reactions of ionised GeH_4 have been investigated by using high-pressure ion-trap mass spectrometry (MS).[17, 18] The thermochemistry of some of the simpler reactions

[a] Prof. Dr. H. Schwarz, Dipl.-Chem. N. Sändig, Dipl.-Chem. M. Diefenbach, Dr. Detlef Schröder
Institut für Organische Chemie
Technische Universität Berlin, Strasse des 17. Juni 135
10 623 Berlin (Germany)
E-mail: schw0531@www.chem.tu-berlin.de

[b] Dr. P. Jackson
Mass Spectrometry Unit
Research School of Chemistry, Australian National University
Canberra ACT 0200 (Australia)
E-mail: jackson@rsc.anu.edu.au

[c] Dr. R. Srinivas
Mass Spectrometry Centre
Indian Institute of Chemical Technology
Hyderabad 500007 (India)
E-mail: srini@iict.ap.nic.in

  0947-6539/01/0701-0151 $ 17.50+.50/0

observed in the MS studies, such as neutral and ionic decompositions for $GeH_n^{0/+}$ ($n = 2,3$) and various Ge–H bond strengths, have been evaluated theoretically using the G1 method[19, 20] and at the multireference configuration interaction (MRSDCI/CASSCF) level.[21]

The theoretical results presented demonstrate that at least some of the widely held assumptions regarding ground state structure of $[Ge,H_2]^+$ might be incorrect, and reexamination might be useful. Moreover, the experimental results reveal new processes for germanium hydride ions, hitherto undescribed in the literature. Where possible, calculations are used to support or refute our proposals based on the experimental results.

Experimental Section and Computational Methods

For a detailed description of the experiment and the instrument used, the reader is advised to consult the review by Schalley et al.[22] and references therein. Briefly, the experiments were performed by using a four-sector modified HF-ZAB AMD 604 mass spectrometer with BEBE configuration,[23] where B and E represent magnetic and electric sectors respectively. $GeH_n^{-/+}$ ($n = 2,3$) were generated by chemical ionisation (CI) of GeH_4 (Union Carbide). Under these conditions, GeH_4 is capable of acting as its own CI gas, that is to say, $GeH_4^{-/+}$ ions are metastable and react with other neutral compounds by proton/hydrogen transfer pathways. Typical source conditions are as follows: pressure about 10^{-4} mbar, source temperature 200 °C, trap current 100 μA, repeller voltage near 0 V, ion extraction voltage 8 kV, $m/\Delta m \geq 1500$. Collisional activation (CA) of B(1)/E(1)-mass selected GeH_n^+ was effected in collision cells positioned between E(1) and B(2) using He as a target gas. In all collision experiments, the target gas pressure was maintained such that, after transiting, 80% of the parent ion beam was recovered. This corresponds to an average of 1.1 – 1.2 collisions per ion.[24] CA products were recorded by scanning the second magnetic sector B(2). Metastable ion (MI) dissociations of GeH_n^+ were monitored for B(1)/E(1)-mass selected ions in a similar experiment, but with the collision cells devoid of gas ($p < 2-3 \times 10^{-9}$ mbar).

Neutralisation-reionisation (NR) and charge reversal (CR) experiments were performed with B(1)/E(1)-mass selected ions, by utilising the dual collision cells between sectors E(1) and B(2). Cation neutralisation was achieved by collision with Xe at 80% transmittance, while reionisation to cations was achieved by collision of the neutrals with O_2, again at 80% transmittance; according to the charges of the projectile and product ions this is referred to as $^+NR^+$. For $^-CR^+$ and $^-NR^+$ experiments, O_2 was the target used throughout. Any ions remaining after the first collision event in the NR experiments were deflected from the primary neutral beam using an electrode maintained at a high voltage (2 kV) positioned before the second collision cell. In order to detect a reionisation signal, the neutral species must be stable for approximately at least a few microseconds. NR- and CR-MS spectra were averaged over 100 acquisitions in order to obtain sufficient S/N ratios, while CA spectra were averaged over 20 – 50 acquisitions. NIDD spectra were derived from quantitative analysis of the $^-NR^+$ and $^-CR^+$ spectra as described previously (NIDD = neutral and ion decomposition difference).[25] In the NIDD scheme, fragmentations occurring at the neutral stage appear as positive signals, while processes of the ionic species give rise to negative peaks.

Density functional calculations[26] for $[Ge,H_2]^{-/0/+}$ were performed by using the Gaussian 94 software[27] on IBM RS/6000 computers running AIX 4.2.1. The structures were investigated as follows: first, geometry optimisations were performed using the 3-parameter hybrid density functional method of Becke (B3LYP)[28–30] in conjunction with basis sets of triple-zeta quality.[31–34] The respective basis sets were supplemented with single p and d functions for Ge, and one s and one p function for H (6 – 311 ++ G(d,p)). The nature of each stationary point located at this level of theory was then established by subsequent frequency analysis. Vertical detachment, ionisation, and recombination energies (VDEs, VIEs, VREs, respectively) were derived from single-point calculations using optimised geometries of relevant minima. We have also reoptimised the structures of $GeH_2^{-/0/+}$ using B3LYP in conjunction with the triple-zeta, correlation-consistent basis sets.[35–37] These results confirm that, at least using the hybrid DFT method, the smaller triple-zeta basis set suffices for an investigation of the chemistry of germanium hydride molecules and ions. As precautionary measures (particularly for the anions), reoptimisations at the CCSD(T)/6 – 311 ++ G(d,p) level have been performed and single point energies obtained for these structures using CCSD(T,full)/cc-pVTZ calculations. The relative energies of the three lowest energy cation structures were also investigated using internally-contracted multireference configuration interaction (IC-MRCI) and averaged coupled-pair functional (MR-ACPF) calculations. The active space comprised the Ge(3d4s4p) and H(1s) orbitals. The multireference calculations were performed on a CRAY-YMP supercomputer using the MOLPRO 96 suite of programmes.[38]

Results and Discussion

This report is divided into two sections, with the results for the dihydride and trihydride species discussed separately. We conclude each section with a discussion of the NIDD spectra, and the implications of our results for earlier experimental measurements. We have refrained from an extended comparison of theoretically derived and experimental spectroscopic constants for $[Ge,H_2]^{-/0/+}$ and direct the interested reader to the relevant literature.[7, 10, 15, 19–21, 39]

$[GeH_2]^{-/0/+}$

The collisional activation spectrum of $^{70}GeH_2^+$ with He as the target gas holds no surprises (Figure 1), other than perhaps the relative abundances of the fragment peaks (m/z 71: m/z 70 $\approx$ 0.62:1.00). That is, loss of H_2 appears to be more favourable than loss of H. This suggests that either a side-on or an end-on isomer, $Ge(H_2)^+$, is formed in large amounts in the CI source, or interconversion between the inserted structure $HGeH^+$

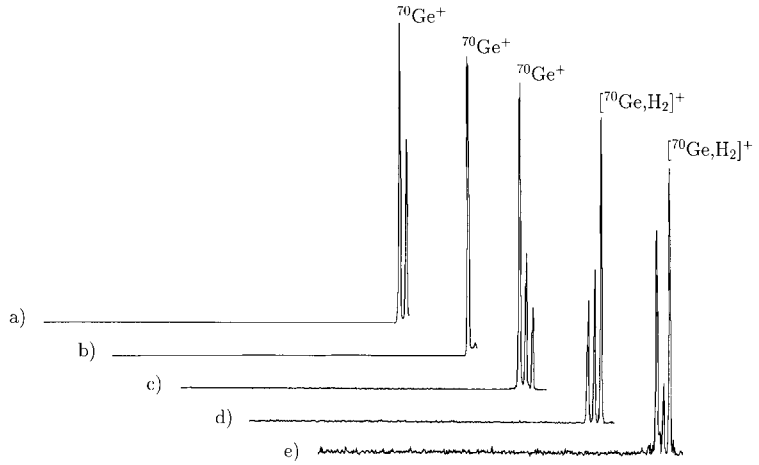

Figure 1. Spectra for $[Ge,H_2]^{+/-}$ ions generated by the chemical ionisation of GeH_4. a) CA mass spectrum. b) MI mass spectrum. c) $^+NR^+$ mass spectrum; the parent peak at m/z 72 is also due to interferent $^{72}Ge^+$. d) $^-CR^+$ mass spectrum. e) $^-NR^+$ mass spectrum.

0947-6539/01/0701-0152 $ 17.50+.50/0 *Chem. Eur. J.* **2001**, *7*, No. 1

and either kind of $Ge(H_2)^+$ isomer is facile. Frontier orbital considerations suggest end-on approach of the dihydrogen will result in formation of $^1\Sigma$ GeH^+ and ^2S H as a H_2 σ/Ge $4p_z$ donation will weaken the H_2 bond, and Ge 4s/H_2 σ^* interaction will have a similar effect. Without recourse to theoretical calculations, it is impossible to arrive at definitive answers concerning the relative abundances of the side-on and inserted isomers.

To further investigate the possible existence of a side-on ion–molecule complex $Ge(H_2)^+$, we have monitored the metastable ion decay of the mass-selected parent ion beam on the microsecond time scale. This spectrum is also presented in Figure 1 and can be regarded as confirmation of the presence of an ion–molecule complex, in that loss of H_2 prevails over that of H atom by more than an order of magnitude (*m*/*z* 71: *m*/*z* 70 ≈1:22). Once again, however, the ratio of the ion molecule complex to the inserted structure is unclear. All previous theoretical studies[18–21] have considered only the inserted isomers, while it is clear from this spectrum that the IM-complex very likely also plays a role.

Given that the stability of neutral GeH_2 is firmly established,[13] the $^+NR^+$ spectrum of $^{70}GeH_2^+$ is useful only for the relative fragment ion abundances (*m*/*z* 70: *m*/*z* 71). This is especially true considering the parent peak is isobaric with $^{72}Ge^+$. In the $^+NR^+$ experiments, a significant fraction of the survivor signal (if not all) will be attributable to $^{72}Ge^+$, but of course this contaminant cannot give rise to fragment peaks. We did not select $^{76}GeH_2^+$ for analysis as *m*/*z* 78 is contaminated with metastable $^{74}GeH_4^+$ and (possibly) small amounts of $^{73}GeH_5^+$. Thus, our discussion of the $^+NR^+$ spectrum is limited to relative ion–neutral geometries and Franck–Condon overlap between the initial and final states.

Thus, the relatively small survivor peak in Figure 1c indicates that most of the $^{70}GeH_2^+$ undergoes fragmentation (recovery signal is 15% of the total ion current), as either a metastable on the neutral surface during the first transition, or on the cation surface after the reionisation event. The small survivor signal is not surprising *if* a large fraction of the parent ion exists as $Ge(H_2)^+$, as ion–molecule complexes rarely survive vertical neutralisation because of the removal of the electrostatic component of the bonding. In any case, the neutral complex $Ge(H_2)$, if it is bound at all, would reside in a very shallow minimum, because H_2 has no dipole moment and a very low polarisability. The base peak in the $^+NR^+$-spectrum corresponds to loss of H_2 (60% total ion current), which again lends credence to our proposal that a significant fraction of $[^{70}Ge,H_2]^+$ exists as $Ge(H_2)^+$.

In both the $^-CR^+$ and $^-NR^+$ spectra of $[^{70}Ge,H_2]^-$, the base peak corresponds to the survivor signal. Analysis of the isotopomer distribution in the CI source reveals that the contribution of $^{72}Ge^-$ to the peak at *m*/*z* 72 is negligible, so we can assume that Franck–Condon factors must be quite favourable for anionic GeH_2^- during both direct two-electron transfers and single-electron transfers (via the neutral surface) to the cation surface. Indeed, this can be directly investigated using ab initio methods, and the results of the $[Ge,H_2]^{-/0/+}$ study are discussed in the following paragraphs.

A schematic diagram of the potential energy surfaces of $[Ge,H_2]^{-/0/+}$ calculated at the CCSD(T,full)/cc-pVTZ//CCSD(T)/6–311++G(d,p) level is presented in Figure 2. The surfaces are zero-point-energy corrected using scaled vibrational frequencies determined using density functional theory (B3LYP/6–311++G(d,p)). A comparison of B3LYP energetics calculated by using the cc-pVTZ and 6–311++G(d,p) basis sets (Table 1) suggests the smaller

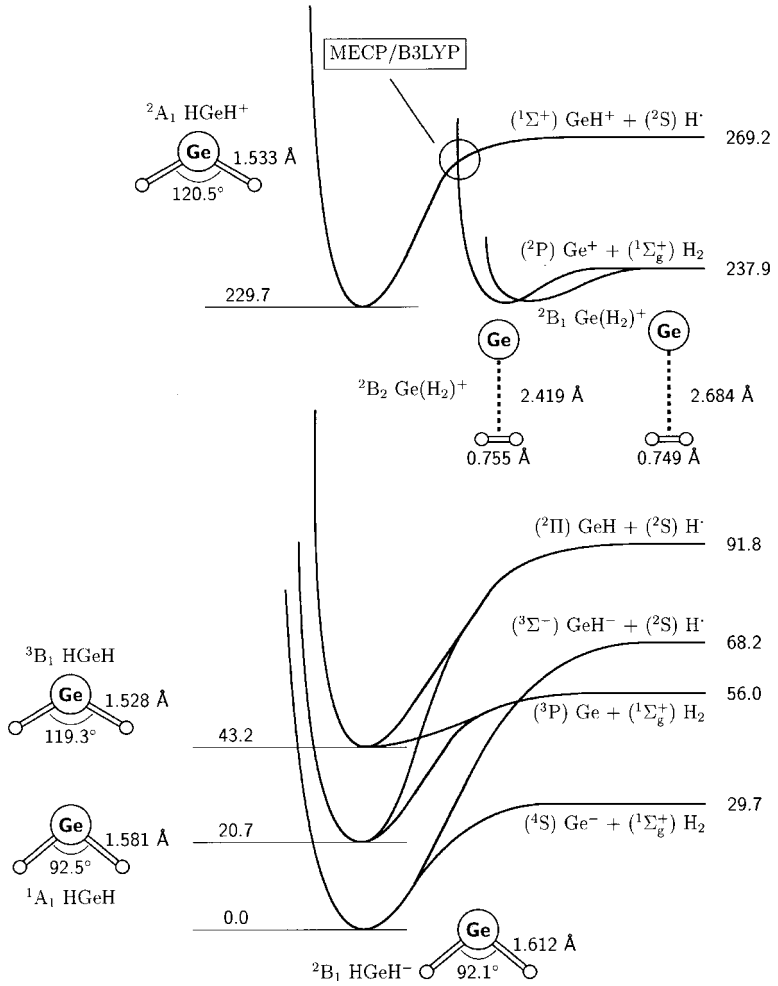

Figure 2. Potential energy surfaces for $[Ge,H_2]^{-/0/+}$ calculated at the CCSD(T,full)/cc-pVTZ//CCSD(T)/6–311++G(d,p) level of theory. Note that, except for the encircled region (Minimum Energy Crossing Point, MECP) discussed in the text, all other crossings are tentative. Relative energies are in kcal mol^{-1}.

Table 1. B3LYP and CCSD(T) energies and geometries for $[Ge,H_2]^{-/0/+}$ and various fragments. The coupled-cluster SCF energies are from single-point CCSD(T,full)/cc-pVTZ//CCSD(T)/cc-pVTZ calculations. IC-MRCI/cc-pVTZ//CCSD(T)/6–311++G(d,p) energies for the three lowest energy isomers of $[Ge,H_2]^+$ are also given.

		E [Hartree]	E_{rel} [kcal mol^{-1}]	r_{GeH} [Å]	r_{HH} [Å]	θ_{HGeH} [°]	ZPE [kcal mol^{-1}]
$^2B_1$ HGeH$^-$	B3LYP/6-311++G(d,p)	−2078.18117	0.0	1.623		91.3	6.2
	B3LYP/cc-pVTZ	−2078.27268	0.0	1.628		91.3	
	CCSD(T)	−2076.81263	0.0	1.611		92.1	
$^1A_1$ HGeH	B3LYP/6–311++G(d,p)	−2078.14263	24.4	1.591		90.9	6.8
	B3LYP/cc-pVTZ	−2078.23605	23.2	1.597		90.8	
	CSD(T)	−2076.78089	20.1	1.581		92.5	
$^3B_1$ HGeH	B3LYP/6–311++G(d,p)	−2078.10215	50.0	1.538		119.8	7.2
	B3LYP/cc-pVTZ	−2078.19389	49.9	1.545		119.7	
	CCSD(T)	−2076.74590	42.2	1.528		119.3	
$^3A_2$ Ge(H_2)	B3LYP/6–311++G(d,p)	−2078.09293	55.8	2.276	0.761	19.3	7.2
	B3LYP/cc-pVTZ	−2078.18939	52.7	2.234	0.764	19.7	
	CCSD(T)	unbound					
$^2B_2$ Ge(H_2)$^+$[a]	B3LYP/6–311++G(d,p)	−2077.81284	233.1	2.185	0.770	20.3	7.3
	B3LYP/cc-pVTZ	−2077.90866	230.4	2.234	0.773	20.4	
	CCSD(T)	−2076.44476	232.8	2.448	0.755	17.7	
	IC-MRCI	−2076.25395	5.0[b]				
$^2B_1$ Ge(H_2)$^+$[a]	B3LYP/6–311++G(d,p)	−2077.80940	235.3	2.407	0.757	18.1	7.3
	B3LYP/cc-pVTZ	−2077.90527	230.6	2.365	0.758	18.4	
	CCSD(T)	−2076.44138	234.9	2.710	0.749	15.9	
	IC-MRCI	−2076.25387	4.8[b]				
$^2A_1$ HGeH$^+$[a]	B3LYP/6–311++G(d,p)	−2077.81096	234.3	1.548		120.3	7.1
	B3LYP/cc-pVTZ	−2077.90187	234.7	1.558		120.3	
	CCSD(T)	−2076.45116	228.8	1.533		120.5	
	IC-MRCI	−2076.26147	0.0[b]				
$^4A_2$ HGeH$^+$	B3LYP/6–311++G(d,p)	−2077.69407	305.7	1.758		79.0	3.7
	B3LYP/cc-pVTZ	−2077.77111	314.7	1.759		78.5	
	CCSD(T)	−2076.32091	308.6	1.682		73.5	

triple-zeta basis set suffices at this level for the cations and neutral compounds, although there are additional problems concerning low-lying electronic states on the ground state cation surface. That is, a proper multireference CI treatment of the three cation states (separated by only 2.2 kcal mol^{-1} at B3LYP/6–311++G(d,p)) is necessary to resolve the global minimum. It is perhaps significant that none of the other theoretical studies of $[Ge,H_2]^+$ have even considered the possible existence of Ge(H_2)$^+$, yet our experimental results strongly point to their existence. Moreover, two electronic states of this complex were located during the B3LYP investigations, although spurious minima can arise through exchange–correlation grid inadequacies, and the Ge–H bond length in $^2B_1$ Ge(H_2)$^+$ does seem extraordinarily long.

In addition to reservations regarding the true cation ground state, which warrants reexamination at a multireference level of theory (see below) and the existence of the $^2B_1$ state of Ge(H_2)$^+$, DFT results for anions should always be viewed cautiously. This is for the following reason: It has been argued in the past that all anions should be unbound at the pure density functional level of theory, with boundedness resulting from basis set incompleteness.[40] To evaluate how this might affect the theoretical electron affinity of GeH_2, some insight can be gained through evaluation of electron affinity (Ge) at various DFT levels (see Table 2) and a comparison with the experimental values.[41] On the basis of this information, we conclude that the errors for B3LYP/6–311++G(d,p) are not large; note, however, that the larger cc-pVTZ basis set gives consistently lower electron affinities for all DFT approaches.

Given that DFT has performed, or will perform, poorly in some instances for the anion and cation, the surfaces important to this study have been recalculated at the CCSD(T)/cc-pVTZ//CCSD(T)/6–311++G(d,p) level of theory using the B3LYP geometries as initial guesses, and in addition, single-point internally contracted multireference configuration interaction calculations, IC-MRCI/cc-pVTZ//CCSD(T)/6–311++G(d,p), and averaged coupled-pair functional calculations, MR-ACPF/cc-pVTZ//CCSD(T)/6–311++G(d,p), have been performed for the three lowest minima located on the cation doublet surface. These results appear alongside the density functional and coupled cluster results in Table 1. Before discussing the bond strengths and other useful data, it is pertinent to review the anion, neutral, and cation potential-energy surfaces at the CCSD(T,full)/cc-pVTZ//CCSD(T)/6–311++G(d,p) level of theory (Figure 2), and the vertical versus adiabatic transition energies calculated for selected minima (from $v=0$) located at this

Table 2. Electron affinity in kcal mol^{-1} of Ge atom at various DFT levels.

	BLYP	BPW91	PW91PW91	G96PW91	B3LYP	BHLYP	B1LYP	exp.
6–311++G(d,p)	27.8	32.7	33.7	32.2	30.6	26.5	27.0	28.7
cc-pVTZ	20.6	27.5	27.8	28.1	24.8	21.7	21.1	

0947-6539/01/0701-0154 $ 17.50+.50/0 *Chem. Eur. J.* **2001**, *7*, No. 1

Table 1. (Continued)

(cont)		E [Hartree]	E_{rel} [kcal mol^{-1}]	r_{GeH} [Å]	r_{HH} [Å]	θ_{HGeH} [°]	ZPE [kcal mol^{-1}]
$^4\Sigma_u^+$ HGeH$^+$[c]	B3LYP/6–311++G(d,p)	–2077.57774	378.7	1.651		180.0	9.5
^{2}S H[c]	B3LYP/6–311++G(d,p)	–0.50226					
	B3LYP/cc-pVTZ	–0.50216					
	CCSD(T)	–0.49981					
$^1\Sigma_g^+$ H_2	B3LYP/6–311++G(d,p)	–1.17957			0.744		6.3
	B3LYP/cc-pVTZ	–1.18000			0.743		
	CCSD(T)	–1.17234			0.744		
^{4}S Ge$^-$	B3LYP/6–311++G(d,p)	–2076.97810					
	B3LYP/cc-pVTZ	–2077.04453					
	CCSD(T)	–2075.59314					
^{3}P Ge[c]			EA [kcal mol^{-1}][d]	IE [kcal mol^{-1}][e]			
	B3LYP/6–311++G(d,p)	–2076.90985	30.6	180.6			
	B3LYP/cc-pVTZ	–2077.00500	24.8	182.0			
	CCSD(T)	–2075.55123	26.3	181.9			
^{2}P Ge$^+$[c]	B3LYP/6–311++G(d,p)	–2076.62207					
	B3LYP/cc-pVTZ	–2076.71492					
	CCSD(T)	–2075.26140					
$^3\Sigma^-$ GeH$^-$	B3LYP/6–311++G(d,p)	–2077.56341		1.633			2.4
	B3LYP/cc-pVTZ	–2077.65611		1.638			
	CCSD(T)	–2076.19815		1.621			
$^2\Pi$ GeH[c]	B3LYP/6–311++G(d,p)	–2077.52295		1.598			2.7
	B3LYP/cc-pVTZ	–2077.61763		1.605			
	CCSD(T)	–2076.16092		1.588			
$^1\Sigma^+$ GeH$^+$[c]	B3LYP/6–311++G(d,p)	–2077.25461		1.592			2.9
	B3LYP/cc-pVTZ	–2077.33088		1.591			
	CCSD(T)	–2075.87859		1.584			

[a] At the ACPF/cc-pVTZ//CCSD(T)/6–311+G(d,p) level, $^2B_2$ Ge(H$_2$)$^+$ is the ground state by a mere 0.6 kcal mol^{-1}; E [Hartree] $^2B_2$ Ge(H$_2$)$^+$ = –2076.38901, $^2A_1$ HGeH$^+$ = –2076.38805, $^2B_1$ Ge(H$_2$)$^+$ = –2076.38560. [b] For the IC-MRCI results, E_{rel}($^2A_1$ HGeH$^+$) has been set to 0.0 kcal mol^{-1}. [c] B3LYP/6–311++G(d,p) results taken from ref. [45]. [d] Experimental value: EA = 28.7 kcal mol^{-1}.[41] [e] Experimental value: IE = 182.2 kcal mol^{-1}.[46]

level (Table 3). These transition energies were calculated by using density functional theory.

According to the calculations, $^2B_1$ HGeH$^-$ is the global minimum for the anion. No ion–molecule complexes were located on either the doublet or quartet surfaces, and all linear isomers were found to be significantly higher in energy. Inspection of Figure 2 reveals that the lowest energy dissociation asymptote corresponds to loss of dihydrogen, which requires 29.7 kcal mol^{-1}. Adiabatic dissociation to ^{4}S Ge$^-$ + $^1\Sigma_g$ H_2 is not possible from the global minimum, thus the lowest fission energy corresponds to loss of atomic hydrogen, which costs 68.2 kcal mol^{-1}. This is much greater than the energy required to detach the electron from $^2B_1$ HGeH$^-$, (electron affinity (GeH$_2$), B3LYP/6–311++G(d,p) = 25.6 kcal mol^{-1}, CCSD(T,full)/cc-pVTZ//CCSD(T)/6–311++G(d,p) = 20.7 kcal mol^{-1}). The experimental value determined by Lineberger and co-workers[41] is 25.5 kcal mol^{-1}, so the B3LYP value is in excellent agreement with experiment in this instance, probably as a result of the fortuitous cancellation of errors, especially given the discrepancy between the experimental and B3LYP/6–311++G(d,p) values for the electron affinity of Ge.

The difference between the vertical and adiabatic detachment values for the transition to the singlet surface is relatively small (Table 3), so that the first collision in either a two-step $^-$CR$^+$ or $^-$NR$^+$ process results in energy deposition to a low vibrational level on the singlet surface, probably v = 0. As all transitions $\Delta S = \pm 1/2$ are allowed, we have also investigated vertical detachment to the triplet neutral surface. In contrast to the favourable Franck–Condon factors which result in the formation of a relatively cool singlet neutral after vertical detachment of $^2B_1$ HGeH$^-$, transitions to the triplet surface deposit some 12 kcal mol^{-1} into the neutral. This is below the calculated D($^3B_1$ HGe–H) bond fission energy (48.6 kcal mol^{-1}), but very close to the asymptote corresponding to the spin-allowed dissociation into ^{3}P Ge + $^1\Sigma_g$ H_2. Given that dissociation via this asymptote will require molecular rearrangement from HGeH to Ge(H$_2$), and thus an orbital crossing on the triplet surface (from B_1 to A_2 according to B3LYP/6–311++G(d,p)), the

Table 3. Relative energies for vertical versus adiabatic transitions calculated at the B3LYP/6–311++G(d,p) level. E_{SP} is total energy of product at reactant geometry.

Transition	Type	E_{SP} [Hartree]	E_v [kcal mol^{-1}]	ΔE_{v-a} [kcal mol^{-1}]
$^2B_1$ HGeH$^- \rightarrow$ $^1A_1$ HGeH	detachment	–2078.14033	25.63	1.5
$^2B_1 \rightarrow$ HGeH$^- \rightarrow$ $^3B_1$ HGeH	detachment	–2078.08247	61.94	12.5
$^2B_1$ HGeH$^- \rightarrow$ $^2A_1$ HGeH$^+$	charge reversal	–2077.79114	244.75	12.6
$^1A_1$ HGeH $\rightarrow$ $^2A_1$ HGeH$^+$	ionisation	–2077.79428	218.59	10.6
$^3B_1$ HGeH $\rightarrow$ $^2A_1$ HGeH$^+$	ionisation	–2077.81089	182.77	< 0.1
$^3A_2$ Ge(H$_2$) $\rightarrow$ $^2B_2$ Ge(H$_2$)$^+$	ionisation	–2077.81262	175.90	0.1
$^2A_1$ HGeH$^+ \rightarrow$ $^1A_1$ HGeH	recombination	–2078.12288	–195.73	12.5
$^2A_1$ HGeH$^+ \rightarrow$ $^3B_1$ HGeH	recombination	–2078.10208	–182.68	< 0.1
$^2B_2$ Ge(H$_2$)$^+ \rightarrow$ $^3A_2$ Ge(H$_2$)	recombination	–2078.09278	–175.67	< 0.1
$^2B_2$ Ge(H$_2$)$^+ \rightarrow$ $^1A_1$ HGeH	recombination	–2078.06359	–157.35	50.1

relative energy of the crossing point, and thus the rate of internal conversion, will largely determine the likelihood of fragmentation. This point was located by manually scanning the potential energy surface while maintaining C_{2v} symmetry,[42] until a geometry was located at which the states were essentially degenerate ($\Delta E_{SCF}\,|\,^3B_1 - {}^3A_2\,| < 0.02$ kcal mol^{-1}). The classical barrier for the interconversion is 40.0 kcal mol^{-1} above $^3B_1$ HGeH. The bond length and the bond angle at which the two states are isoenergetic are $r_e = 1.645(8)$ Å, $\theta_{HGeH} = 65.02(3)^\circ$. Thus, the energy imparted by the transition from the anion still appears to be insufficient to cause dissociation via this asymptote; however, we will not discount this completely, as coupling between sufficiently anharmonic vibrational states may lead to tunneling and dissociation, either directly (CCSD(T), see Table 1) or via excited $^3A_2$ Ge(H_2), which, of course, will dissociate as it is bound by a mere 1.4 kcal mol^{-1}.

We now turn our attention to the cation surfaces. Inspection of Figure 2 reveals that the cation situation is distinct from those encountered for the neutral or anion; that is, three structures are very close in energy, and at the level of theory applied, it remains unclear which is indeed the global minimum. Two of these structures are ion–molecule complexes, $^2B_2$ Ge$(H_2)^+$ and $^2B_1$ Ge$(H_2)^+$; the latter is probably an encounter complex.

According to B3LYP/6–311++G(d,p) calculations, the cation global minimum is $^2B_2$ Ge$(H_2)^+$, and the inserted structure on this surface ($^2A_1$) is 1.2 kcal mol^{-1} less stable. With the bigger basis set, the B3LYP energy difference between the $^2B_2$ and $^2A_1$ states increases to 4.3 kcal mol^{-1}, but the situation is reversed at the CCSD(T,full)/cc-pVTZ//CCSD(T)/6–311++G(d,p) level, with $^2A_1$ HGeH$^+$ more stable than $^2B_2$ Ge$(H_2)^+$ by 4.0 kcal mol^{-1}. Clearly, this is a problem that must be resolved by using higher levels of theory; in an effort to see how the relative energies vary with increasingly sophisticated calculations, MR-ACPF/cc-pVTZ//CCSD(T)/6–311++G(d,p) and IC-MRCI/cc-pVTZ//CCSD(T)/6–311++G(d,p) single-point energies were obtained for each of the three low-lying cation states. Again, the results are ambiguous with the MRCI calculations favouring the inserted structure, whereas the MR-ACPF calculations favour the ion–molecule complex. Without geometry optimisations at these computationally expensive levels as well as consideration of spin-orbit effects, the cation global minimum cannot be unequivocally established; nevertheless, the present results establish that both isomers are important for the cationic species.

All three cation minima are shallow with respect to the ^2P Ge$^+$+$^1\Sigma_g^+$ H_2 asymptote, which is only 8.2 kcal mol^{-1} above $^2A_1$ HGeH$^+$ according to CCSD(T,full)/cc-pVTZ//CCSD(T)/6–311++G(d,p). The energies of the minima on the ground state surface with respect to this asymptote conveniently explains the high abundance of the H_2-loss signals in the MI and CA spectra of $[^{70}Ge,H_2]^+$.

There are no spin barriers on the ground state cation surface that hinder dissociation either via loss of H or H_2, although loss of H_2 by the inserted structure will again proceed via internal conversion to either $^2B_1$ or $^2B_2$ states of Ge$(H_2)^+$. In a method analogous to that previously applied[42] to locate the crossing point on the triplet neutral surface, the point of intersection between the inserted and ion–molecule structures on the cation surface was also found. The classical barrier for this process is 38.1 kcal mol^{-1} (B3LYP/6–311++G(d,p)) which is very close to the dissociation limit $^1\Sigma^+$ GeH$^+$+^{2}S H (this point is above this asymptote at the B3LYP/6–311++G(d,p) level). The structure at the crossing point is: $r_e = 1.673(4)$ Å, $\theta_{HGeH} = 68.84(4)^\circ$, ($\Delta E_{SCF}\,|\,^2B_2 - {}^2A_1\,| < 0.02$ kcal mol^{-1}). The close proximity of the crossing point to the H-loss exit channel (41.9 kcal mol^{-1} above $^2A_1$ HGeH$^+$) suggests both processes will be competitive, with a small fraction of the ions interconverting and then dissociating via the $^1\Sigma^+$ GeH$^+$+^{2}S H exit channel. Once again, theory is able to account for the H-loss peak detected in the MI spectrum of $[^{70}Ge,H_2]^+$.

Now that we have elicited an appreciation of the dissociation requirements for the cation surface and have explained some of the observed experimental phenomena, we are in a position to discuss the consequences of ionisation events that have been probed experimentally. Noting the significant difference in the bond angles of $^1A_1$ HGeH and $^2A_1$ HGeH$^+$, it is not surprising that the difference between the vertical and adiabatic ionisation energies of $^1A_1$ HGeH is 10.6 kcal mol^{-1} (Table 3). The situation is quite different for $^3B_1$ HGeH, with near coincident adiabatic and vertical ionisation energies, which suggests low vibrational states of $^2A_1$ HGeH$^+$, most probably $v = 0$, will be populated by vertical ionisation from the triplet precursor.

If we now recall that $^-$CR$^+$ can be a two-step as well as a one-step process, and assuming that the parent anion $^2B_1$ HGeH$^-$ is formed in low vibrational states, it is unlikely that the collisional electron detachment generates large amounts of $^3B_1$ HGeH from simple thermochemical considerations. If $^3B_1$ HGeH is formed, it will be in a high vibrational state (Franck–Condon overlap for the $^2B_1$ HGeH $\rightarrow$ $^3B_1$ HGeH is poor), so whichever transitions dominate, it is likely that the inserted cation that is formed will be vibrationally excited. According to our calculated crossing point, the inserted cation does not possess the requisite energy to dissociate by loss of H_2 after vertical ionisation from $^1A_1$ HGeH. Likewise, single-step charge reversal results in an inserted cation with 12.6 kcal mol^{-1} internal energy, which again is insufficient for this process, unless either an oblique collisional activation mechanism is invoked (small impact parameter with vibrational, accompanying electronic excitation), or there is quantum tunneling arising from vibronic coupling.

The poor Franck–Condon overlap between $^2A_1$ HGeH$^+$ and $^1A_1$ HGeH is manifested in the calculated (internal) energy imparted to the neutral during recombination from the ground vibrational state of $^2A_1$ HGeH$^+$ (12.5 kcal mol^{-1}, Table 3). Thus, all the cations in, or close to, the zero level should survive recombination to the singlet neutral surface, as the first crossing point is more than 25 kcal mol^{-1} higher in energy. In addition, the Franck–Condon factors for transitions from ground state $^2B_2$ Ge$(H_2)^+$ to $^3A_2$ Ge(H_2) are quite favourable (Δ (RE$_a$ – RE$_v$) < 1 kcal mol^{-1}), and if the calculations are correct, no fragmentation should be observed during $^+$NR$^+$ of ^{2}Ge$(H_2)^+$. Why then, are the H_n loss signals so abundant in the $^+$NR$^+$ spectrum? The explanations provided

0947-6539/01/0701-0156 $ 17.50+.50/0 *Chem. Eur. J.* **2001**, *7*, No. 1

above are feasible, but the CCSD(T) results for $^3A_2$ $Ge(H_2)$ are revealing; no bound, neutral germanium–dihydrogen complex could be located at this level of theory. That is to say, $^3A_2$ $Ge(H_2)$ is a grid artefact of the exchange-correlation quadrature in DFT calculations. Therefore, neutralisation of the ion–molecule complexes $Ge(H_2)^+$ should result only in dissociation.

If the theoretical value for IE(Ge) can be used to gauge the accuracy of IE_v for molecular species (IE(Ge), B3LYP/6–311++G(d,p) = 7.83 eV, IE_{exp} = 7.90 eV,[43, 44] $\Delta E < 2$ kcal mol^{-1}), at the very least a qualitative appreciation of transitions likely to result in dissociation can be gained from the B3LYP calculations. We are still confronted with the problem that with the present software it is still not feasible to calculate vertical IEs for high initial reactant states, as we have no a priori knowledge of the vibrational spacings. This is particularly important for our interpretations regarding two-step $^-CR^+$ processes in which the neutral intermediate is vibrationally excited. Nevertheless, if the probability of the transition to $v = 0$ is poor, the Franck–Condon factors for transitions to higher states must be more favourable, with the probability of system crossing increasing as higher, more anharmonic states are accessed. The higher the final vibrational state, the higher the chance of system crossing.

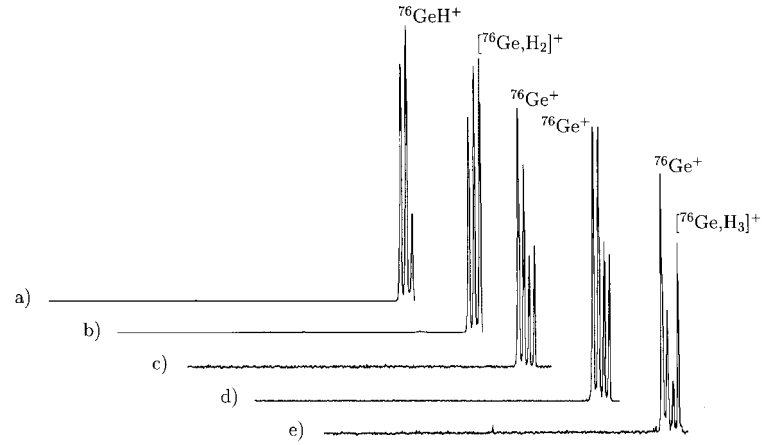

Figure 3. Spectra for $[Ge,H_3]^{+/-}$ ions generated by the chemical ionisation of GeH_4. a) CA mass spectrum. b) MI decomposition mass spectrum. c) $^+NR^+$ mass spectrum. d) $^-CR^+$ mass spectrum. e) $^-NR^+$ mass spectrum.

Finally, let us return to the experimental data by the quantitative analysis of the $^-NR^+$ and $^-CR^+$ spectra in terms of the NIDD scheme.[22, 25] Here, positive intensities are indicative of neutral dissociations, whereas the negative are indicative of dissociations on the ion surfaces. $^-NIDD^+$ analysis of GeH_2^- yields a positive signal (17%) for the Ge^+ fragment and a negative one (−14%) for GeH^+; the recovery signal is almost unchanged. The loss of H, predominantly on the cation surface, is readily rationalised by a comparison of the bond strengths D(HGe$^+$–H), 30.0 kcal mol^{-1}, and D(HGe–H), 70.2 kcal mol^{-1}, which is more than twice this value. What is unusual is that many of the neutrals formed during the two-step $^-NR^+$ process possess the energy to overcome what appears to be a significant internal conversion barrier. Whether the anions formed in the CI source are electronically or vibrationally excited is open to speculation, but it appears as though either an oblique collisional activation mechanism or vibronic-coupled tunneling is operative.

$[Ge,H_3]^{-/0/+}$

The MI spectrum of the trihydride cation $[^{76}Ge,H_3]^+$ is presented in Figure 3; contributions from isobaric species are negligible due to the non-existence of ^{75}Ge. Losses of H_n, $n = 1–3$, are prominent; particularly surprising is the high intensity of H loss ($n = 1$). Noting that internal conversion for $[Ge,H_2]^+$ appears to be facile, the spectra of $[Ge,H_3]^+$ will therefore be complicated by the superposition of the subsequent decompositions of $[Ge,H_2]^+$. It is possible to determine, using the MI spectrum of CI-generated GeH_2^+, approximate branching ratios of GeH_3^+ if some simple assumptions are made, namely 1) the peak at m/z 76 in the trihydride MI spectrum is entirely due to decompositions of the product $^{76}GeH_2^+$, as concerted loss of H_3 is unlikely, and 2) the metastable behaviour of the $[Ge,H_3]^+$-decomposition product GeH_2^+ equals that of CI-generated GeH_2^+. This, of course, is a tenuous assumption, as a fraction of CI-generated GeH_2^+ might be formed by direct electron ionisation of GeH_2, although at the pressures maintained in the CI source, this should only be a small fraction of the ions detected downstream. Nevertheless, these ions might constitute the metastable component of the ion beam. Fortunately, the errors that will be introduced by this approximation will, in any case, be small (see below).

The Ge^+ fragment represents 30% of the metastable ion products, while 35% of GeH_2^+ formed from metastable $[Ge,H_3]^+$ does not dissociate before reaching the detector. Using the ratio of 1:22 (vide supra), the GeH^+ ion current can be adjusted for decompositions arising from GeH_2^+. The metastable ion decomposition scheme is given in Equation (2). The percentages for $[Ge,H_3]^+$ are only for those ions that react between the source and detector, whereas those for $[Ge,H_2]^+$ can be summed to give an approximate percentage of metastable GeH_2^+ product ions that dissociate before reaching the detector. Given that source pressures can have pronounced effects on the metastable ion current, the ratios presented will be extremely sensitive to this variable and the ion internal energy.

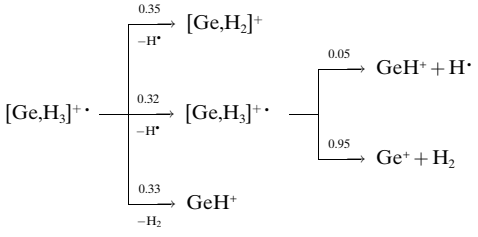

(2)

Table 4. B3LYP energies and geometries for $[Ge,H_3]^{-/0/+}$.

		E [Hartree]	E_{rel} [kcal mol^{-1}]	ZPE [kcal mol^{-1}]	r_{GeH} [Å]	θ_{HGeH} [°]	θ_{oop} [°][a]
$^1A_1$ GeH_3^-	(C_{3v})	−2078.82192	0.0	11.1	1.616	93.7	32.6
$^3A_1$ GeH_3^-	(C_{3v})	−2078.74008	51.4	12.1	1.546	110.1	18.8
$^2A_1$ GeH_3	(C_{3v})	−2078.76131	38.0[b]	12.5	1.541	110.8	18.0
$^2A''$ $HGe(H_2)$	(C_s)	−2078.72647	60.4	11.1	1.601 2.132[e] 0.769[f]	81.0[c]	88.4[d]
$^1A_1'$ GeH_3^+	(D_{3h})	−2078.46635	223.1[b]	13.0	1.524	120.0	0.0
$^1A'$ $HGe(H_2)^+$	(C_s)	−2078.44842	234.4	12.0	1.590 2.129[e] 0.773[f]	69.4[c]	0.0[d]
$^3A''$ $HGe(H_2)^+$	(C_s)	−2078.36822	284.7	11.3	1.602 1.903[e] 0.773[f]	102.4[c]	92.6[d]
				BDE [kcal mol^{-1}][g]			
$^2B_1$ GeH_2^-+H$^\cdot$		−2078.68343	86.9	86.9			
$^1A_1$ GeH_2+H$^\cdot$		−2078.64462	111.3	73.2			
$^3A_2$ $Ge(H_2)$+H$^\cdot$		−2078.59519	142.3	82.4			
$^2A_1$ GeH_2^++H$^\cdot$		−2078.31322	319.2	96.1			
$^2B_2$ $Ge(H_2)^+$+H$^\cdot$		−2078.31510	318.0	83.7			
$^3\Sigma^-$ GeH^-+H_2		−2078.74298	49.5				
$^2\Pi$ GeH+H_2		−2078.70252	74.9	15.0			
$^1\Sigma^+$ GeH^++H_2		−2078.43418	243.3	8.9			

[a] Deviation from planarity (i. e. from D_{3h} symmetry). [b] The calculated adiabatic EA(GeH_3) = 1.657 eV and IE(GeH_3) = 8.022 eV agree well with the experimental figures of 1.61 ± 0.12 eV and 7.948 ± 0.005 eV, respectively.[43, 44] [c] Angle to the bond centre of the H_2 unit. [d] Dihedral angle. [e] Distance to the bond centre of the H_2 unit. [f] H–H distance in the dihydrogen unit. [g] Bond energy of second fragment to first fragment.

The CA spectrum of $[Ge,H_3]^+$, once corrected for metastable decompositions, is quite interesting. For instance, after MI adjustment, H loss accounts for only one-tenth of the total fragment-ion current. The most abundant peak once again corresponds to H_2 loss, and it is apparent that $HGe(H_2)^+$ complexes are important to the chemistry of the trihydride cation (Table 4).

While consecutive fragmentations also complicate the interpretation of the $^+NR^+$ spectrum of $[GeH_3]^+$, the mere observation of a recovery signal in conjunction with the negligible role of isobaric interferences obviously implies that the neutral $[Ge,H_3]^0$ radical is stable on a microsecond timescale. Hence, some of the cation states can survive vertical recombination and the subsequent reionisation event. Similarly, the $^-CR^+$ spectrum of $[Ge,H_3]^-$ shows a distinct recovery signal due to the two-electron oxidation of the anionic to the cationic species. Notably, the recovery signal is most abundant in the $^-NR^+$ mass spectrum. These differences result in a $^-NIDD^+$ spectrum of $[Ge,H_3]^-$ in which the losses of H$^\cdot$ and H_2 give rise to negative signals and thus take place predominantly on the cation surface (m/z 78, $I = -10$, m/z 77, $I = -12$), whereas the NIDD signal for the survivor is distinctly positive (m/z 79, $I = 13$); the remaining NIDD peak is Ge^+ (m/z 77, $I = 9$).

In order to shed further light on these experimental results, we briefly examined the $[Ge,H_3]$ system using the B3LYP approach (Table 4). As with $[Ge,H_2]^+$, we find two isomers for the cationic species of which the classical germyl cation GeH_3^+ is, however, by about 10 kcal mol^{-1} more stable than the dihydrogen complex $HGe(H_2)^+$. The same holds true for the neutral and anionic germyl species GeH_3^0 and GeH_3^-, respectively. Irrespective of the charge, the three germyl species $GeH_3^{+/0/-}$ possess a three-fold axis and all are thermodynamically stable with resepct to losses of atomic and/or molecular hydrogen. Of particular interest with respect to the CR and NR experiments in the present context are the geometry differences between the different charge states and the resulting differences between vertical and adiabatic electron transfers. Thus, the germyl anion as well as the neutral have pyramidal structures which may formally be ascribed to sp^3 hybridisation of germanium. The main changes upon electron detachment from GeH_3^- to afford GeH_3^0 concerns the Ge–H bond lengths which decrease by almost 0.1 Å. This difference results in $\Delta E_{v-a} = 13.2$ kcal mol^{-1} for electron detachment in a keV collision (Table 5). Instead, the Ge–H bond lengths are almost unperturbed in the transition from neutral to cationic germyl, while hybridization changes from sp^3 to sp^2, that is formation of a planar germyl cation.

Table 5. Relative energies for vertical versus adiabatic transitions calculated at the B3LYP/6–311++G(d,p) level. E_{SP} is total energy of product at reactant geometry.

Transition	Type	E_{SP} [Hartree]	E_v [kcal mol^{-1}]	ΔE_{v-a} [kcal mol^{-1}]
$^1A_1$ $GeH_3^- \rightarrow$ $^2A_1$ GeH_3	detachment	−2078.74029	51.22	13.2
$^1A_1$ $GeH_3^- \rightarrow$ $^1A_1'$ GeH_3^+	charge reversal	−2078.36794	284.87	61.8
$^2A_1$ $GeH_3 \rightarrow$ $^1A_1'$ GeH_3^+	ionisation	−2078.43727	203.34	18.3
$^2A''$ $HGe(H_2) \rightarrow$ $^1A'$ $HGe(H_2)^+$	ionisation	−2078.44349	177.57	3.1
$^1A_1'$ $GeH_3^+ \rightarrow$ $^2A_1$ GeH_3	recombination	−2078.75285	−179.78	5.3
$^1A'$ $HGe(H_2)^+ \rightarrow$ $^2A''HGe(H_2)$	recombination	−2078.72562	−173.94	0.5

0947-6539/01/0701-0158 $ 17.50+.50/0 *Chem. Eur. J.* **2001**, *7*, No. 1

Again, this change in geometry is associated with a considerable ΔE_{v-a} of 18.3 kcal mol^{-1}. Nevertheless, these amounts of internal energy can still be accomodated by part of the neutral species resulting in the distinct recovery signals in the NR spectra. These computational results can also pleasingly explain the pronounced difference between the intensties of the recovery signals in the $^{-}CR^{+}$ compared to the $^{-}NR^{+}$ and the resulting positive $^{-}NIDD^{+}$ peak for the survivor. Thus, the stepwise NR transition from GeH_3^- to GeH_3^0, which then—after relaxation for about a microsecond—is ionised from GeH_3^0 to GeH_3^+, is associated with much more favourable Franck–Condon factors than the direct, two-electron oxidation of GeH_3^- to GeH_3^+ upon charge reversal. Indeed, $\Delta E_{v-a} = 61.8$ kcal mol^{-1} for anion oxidation to the cation is much larger than the sum of the energies deposited in the germyl species in two single-electron transfer events. Hence, these results nicely confirm the notion that stepwise electron transfer in the NR sequence is a much softer event that direct two-electron transfer upon charge reversal.[22, 25] Finally, the comparably low abundance of the recovery signal in Figure 3c can again be regarded as a hint for the contribution of hydrogen complexes to the mass selected $[Ge,H_3]^+$ beam, because the Franck–Condon factors of the $^{+}NR^{+}$ sequence otherwise do not appear particularly unfavourable.

Conclusion

Theory and experiment demonstrate the existence of germylidene $GeH_2^{-/0/+}$ and germyl $GeH_3^{-/0/+}$ as long-lived molecules, as anions, neutral species, and cations. However, the mass spectrometric results presented in this study imply that $H_nGe(H_2)^+$ complexes ($n = 0,1$) are of central importance in the gas-phase chemistry of cationic germanium hydrides; similarly, $H_nSi(H_2)^+$ species might play a role in silane plasmas. Reappraisal of the true ground state of $[Ge,H_2]^+$ is warranted on the basis of these experimental and computational results. It is not surprising that this is the first observation of $H_nGe(H_2)^+$ as significant difficulties are encountered in accessing the ion–molecule complexes from the neutral species or anions due to poor Franck–Condon factors. On the other hand, this can be advantageous for electronic state selection of the hydride cations.

Internal conversion barriers for $[HGeH \rightarrow Ge(H_2)]^{0/+}$ were calculated at the B3LYP/6–311++G(d,p) level of theory, as well as vertical and adiabatic detachment, recombination, and ionisation energies. The theoretical barrier heights suggest vibronic coupling, resulting in quantum-tunneling, is important for these orbital-forbidden transitions. Neutral GeH_2 is an attractive candidate for laser-spectroscopic experiments to probe 1) the minimum energy crossing point for the singlet–triplet surface, and 2) if it is possible to generate in good yields, the energy onset for photodissociation of $^3B_1$ HGeH yielding H_2. The former experiment will provide information regarding spin-orbit mediated spin transitions, whereas the latter should provide some insight into quantum-tunneling/vibronic coupling.

Acknowledgement

This research was supported by the Deutsche Forschungsgemeinschaft, the Volkswagen-Stiftung, and the Fonds der Chemischen Industrie. The Konrad-Zuse-Zentrum, Berlin, is acknowledged for generous allocation of computer time. R.S. is grateful to the Deutscher Akademischer Austauschdienst (DAAD) for financial support, and would like to thank Dr. K.V. Raghavan, Director of the Indian Institute of Chemical Technology, for his encouragement and assistance.

[1] R. Squires, *Chem. Rev.* **1987**, *87*, 623.
[2] C. L. Collins, K. G. Dyall, H. F. Schaefer, III, *J. Chem. Phys.* **1995**, *102*, 2024.
[3] P. Pyykkö, *Chem. Rev.* **1988**, *88*, 563.
[4] L. G. M. Pettersson, C. W. Bauschlicher, Jr., S. R. Langhoff, H. Partridge, *J. Chem. Phys.* **1987**, *87*, 481.
[5] S. R. Langhoff, C. W. Bauschlicher, Jr., L. G. M. Pettersson, H. Partridge, *J. Chem. Phys.* **1987**, *86*, 268.
[6] K. Balasubramanian, K. S. Pitzer, *Adv. Chem. Phys.* **1987**, *67*, 287.
[7] K. G. Dyall, *J. Chem. Phys.* **1992**, *96*, 1210.
[8] Z. Barandiaran, L. Seijo, *J. Chem. Phys.* **1994**, *101*, 4049.
[9] S. Koseki, M. S. Gordon, M. W. Schmidt, N. Matsunaga, *J. Phys. Chem.* **1995**, *99*, 12764.
[10] D. A. Chapman, J. Li, K. Balasubramanian, S. H. Lin, *J. Chem. Phys.* **1988**, *88*, 3826.
[11] N. N. Greenwood, A. Earnshaw, *The Chemistry of the Elements*, Pergamon Press, Oxford, **1984**.
[12] C. G. Newman, J. Dzarnoski, M. A. Ring, H. E. O'Neal, *Int. J. Chem. Kinet.* **1980**, *12*, 661.
[13] K. Saito, K. Obi, *Chem. Phys. Lett.* **1993**, *215*, 193.
[14] R. Becerra, S. E. Boganov, M. P. Egorov, O. M. Nefedov, R. Walsh, *Chem. Phys. Lett.* **1996**, *260*, 433.
[15] M. A. Ali, Y.-K. Kim, W. Hwang, N. M. Weinberger, M. E. Rudd, *J. Chem. Phys.* **1997**, *106*, 9602.
[16] R. Becerra, S. E. Boganov, M. P. Egorov, V. I. Faustov, O. M. Nefedov, R. Walsh, *J. Am. Chem. Soc.* **1998**, *120*, 12657.
[17] L. Operti, M. Splendore, G. A. Vaglio, P. Volpe, *Organometallics* **1993**, *12*, 4516.
[18] L. Operti, M. Splendore, G. A. Vaglio, A. M. Franklin, J. F. J. Todd, *Int. J. Mass Spectrom. Ion Processes* **1994**, *136*, 25.
[19] R. C. Binning, L. A. Curtiss, *J. Chem. Phys.* **1990**, *92*, 1860.
[20] R. C. Binning, L. A. Curtiss, *J. Chem. Phys.* **1990**, *92*, 3688.
[21] K. K. Das, K. Balasubramanian, *J. Chem. Phys.* **1990**, *93*, 5883.
[22] C. A. Schalley, G. Hornung, D. Schröder, H. Schwarz, *Chem. Soc. Rev.* **1998**, *27*, 91.
[23] C. A. Schalley, D. Schröder, H. Schwarz, *Int. J. Mass Spectrom. Ion Processes* **1996**, *153*, 173.
[24] J. L. Holmes, *Org. Mass Spectrom.* **1985**, *20*, 169.
[25] C. A. Schalley, G. Hornung, D. Schröder, H. Schwarz, *Int. J. Mass Spectrom.* **1998**, *172/173*, 181.
[26] W. Koch, M. C. Holthausen, *A Chemist's Guide to Density Functional Theory*, Wiley-VCH, Weinheim, **2000**.
[27] M. J. Frisch, G. W. Trucks, H. B. Schlegel, P. M. W. Gill, B. G. Johnson, M. A. Robb, J. R. Cheeseman, T. A. Keith, G. A. Petersson, J. A. Montgomery, K. Raghavachari, M. A. Al-Laham, V. G. Zakrzewski, J. V. Ortiz, J. B. Foresman, J. Cioslowski, B. B. Stefanov, N. Nanayakkara, M. Challacombe, C. Y. Peng, P. Y. Ayala, W. Chen, M. W. Wong, J. L. Andres, E. S. Replogle, R. Gomperts, R. L. Martin, D. J. Fox, J. S. Binkley, D. J. DeFrees, J. Baker, J. P. Stewart, M. Head-Gordon, C. Gonzales, J. A. Pople, *Gaussian 94, Rev. E.1*, Gaussian, Pittsburgh, PA, **1994**.
[28] A. D. Becke, *Phys. Rev. A* **1988**, *38*, 3088.
[29] A. D. Becke, *J. Chem. Phys.* **1993**, *98*, 5648.
[30] C. Lee, W. Yang, R. G. Parr, *Phys. Rev. B* **1988**, *37*, 785.
[31] R. Krishnan, J. S. Binkley, R. Seeger, J. A. Pople, *J. Chem. Phys.* **1980**, *72*, 650.
[32] R. C. Binning, L. A. Curtiss, *J. Comput. Chem.* **1990**, *11*, 1206.
[33] L. A. Curtiss, M. P. McGrath, J.-P. Blandeau, N. E. Davis, R. C. Binning, L. Radom, *J. Chem. Phys.* **1995**, *103*, 6104.
[34] M. P. McGrath, L. Radom, *J. Chem. Phys.* **1991**, *94*, 511.

  0947-6539/01/0701-0159 $ 17.50+.50/0

[35] T. H. Dunning, Jr., *J. Chem. Phys.* **1989**, *90*, 1007.
[36] D. E. Woon, T. H. Dunning, Jr., *J. Chem. Phys.* **1993**, *98*, 1358.
[37] D. E. Woon, T. H. Dunning, Jr., unpublished results.
[38] MOLPRO is a package of ab initio programmes written by H.-J. Werner and P. J. Knowles, with contributions from J. Almlöf, R. D. Amos, A. Berning, M. J. O. Deegan, F. Eckert, S. T. Elbert, C. Hampel, R. Lindh, W. Meyer, A. Nicklass, K. Peterson, R. Pitzer, A. J. Stone, P. R. Taylor, M. E. Mura, P. Pulay, M. Schuetz, H. Stoll, T. Thorsteinsson, and D. L. Cooper.
[39] P. M. Mayer, J.-F. Gal, L. Radom, *Int. J. Mass Spectrom. Ion Processes* **1997**, *167/168*, 689.
[40] J. M. Galbraith, H. F. Schaefer, III, *J. Chem. Phys.* **1996**, *105*, 862.
[41] T. M. Miller, A. E. S. Miller, W. C. Lineberger, *Phys. Rev. A* **1986**, *33*, 3558.
[42] J. N. Harvey, M. Aschi, H. Schwarz, W. Koch, *Theor. Chem. Acc.* **1998**, *99*, 95.
[43] *NIST Chemistry WebBook* (Eds.: W. G. Mallard, P. J. Linstrom), NIST Standard Reference Database, no. 69, National Institute of Standards and Technology, Gaithersburg, MD, 20899, **1998**, http://webbook.nist.gov.
[44] S. G. Lias, J. E. Bartmess, J. F. Liebman, J. L. Holmes, R. D. Levin, W. G. Mallard, *Ion Energetics Data*, Mallard and Linstrom,[43] **1998**, http://webbook.nist.gov.
[45] P. Jackson, M. Diefenbach, D. Schröder, H. Schwarz, *Eur. J. Inorg. Chem.* **1999**, 1203.
[46] C. M. Brown, S. G. Tilford, M. L. Ginter, *J. Opt. Soc. Am.* **1977**, *67*, 584.

Received: May 24, 2000 [F2510]

0947-6539/01/0701-0160 $ 17.50+.50/0